Enhanced up-conversion for photovoltaics via concentrating integrated optics

Georgios E. Arnaoutakis,[1] Jose Marques-Hueso,[1] Aruna Ivaturi,[1] Karl W. Krämer,[2] Stefan Fischer,[3] Jan Christoph Goldschmidt,[3] and Bryce S. Richards[1,4,*]

[1] *Institute of Photonics & Quantum Sciences, Heriot-Watt University, Edinburgh, EH14 4AS, United Kingdom*
[2] *Department of Chemistry and Biochemistry, University of Bern, Freiestrasse 3, CH-3012 Bern, Switzerland*
[3] *Fraunhofer - Institute for Solar Energy Systems ISE, Heidenhofstrasse 2, 79110 Freiburg, Germany*
[4] *Present address: Nelson Mandela African Institute of Science and Technology, Tengeru, Arusha, Tanzania*
[*] *B.S.Richards@hw.ac.uk*

Abstract: Concentrating optics are integrated into up-conversion photovoltaic (UC-PV) devices to independently concentrate sub-band-gap photons on the up-conversion layer, without affecting the full solar concentration on the overlying solar cell. The UC-PV devices consist of silicon solar cells optimized for up-conversion, coupled with tapered and parabolic dielectric concentrators, and hexagonal sodium yttrium fluoride (β-$NaYF_4$) up-converter doped with 25% trivalent erbium (Er^{3+}). A normalized external quantum efficiency of $1.75x10^{-2}$ cm^2/W and $3.38x10^{-2}$ cm^2/W was obtained for the UC-PV device utilizing tapered and parabolic concentrators respectively. Although low to moderate concentration was shown to maximize UC, higher concentration lead to saturation and reduced external quantum efficiency. The presented work highlights some of the implications associated with the development of UC-PV devices and designates a substantial step for integration in concentrating PV.

OCIS codes: (190.7220) Upconversion; (160.5690) Rare-earth-doped materials; (040.5350) Photovoltaic; (220.1770) Concentrators; (250.5230) Photoluminescence; (300.6420) Spectroscopy, nonlinear; (350.6050) Solar energy.

References and links

1. W. Shockley and H. J. Queisser, "Detailed balance limit of efficiency of p-n junction solar cells," J. Appl. Phys. **32**(3), 510–519 (1961).
2. A. Richter, M. Hermle, and S. W. Glunz, "Reassessment of the Limiting Efficiency for Crystalline Silicon Solar Cells," IEEE J. Photovoltaics **3**(4), 1184–1191 (2013).
3. T. Trupke, M. Green, and P. Wurfel, "Improving solar cell efficiencies by up-conversion of sub-band-gap light," J. Appl. Phys. **92**(7), 4117–4122 (2002).
4. F. Auzel, "Upconversion and anti-Stokes processes with f and d ions in solids," Chem. Rev. **104**(1), 139–174 (2004).
5. M. Pollnau, D. Gamelin, S. Lüthi, H. Güdel, and M. Hehlen, "Power dependence of upconversion luminescence in lanthanide and transition-metal-ion systems," Phys. Rev. B **61**(5), 3337–3346 (2000).
6. J. Suyver, A. Aebischer, S. García-Revilla, P. Gerner, and H. Güdel, "Anomalous power dependence of sensitized upconversion luminescence," Phys. Rev. B **71**(12), 125123 (2005).
7. A. Ivaturi, S. K. MacDougall, R. Martín-Rodríguez, M. Quintanilla, J. Marques-Hueso, K. W. Kramer, A. Meijerink, and B. S. Richards, "Optimizing infrared to near infrared upconversion quantum yield of β-NaYF4: Er3+ in fluoropolymer matrix for photovoltaic devices," J. Appl. Phys. **114**, 013505 (2013).
8. A. Shalav, B. S. Richards, T. Trupke, K. W. Krämer, and H. U. Gudel, "Application of $NaYF_4:Er^{3+}$ up-converting phosphors for enhanced near-infrared silicon solar cell response," Appl. Phys. Lett. **86**(1), 013505 (2005).
9. B. S. Richards and A. Shalav, "Enhancing the near-infrared spectral response of silicon optoelectronic devices via up-conversion," IEEE Trans. Electron. Dev. **54**(10), 2679–2684 (2007).
10. H. Steinkemper, S. Fischer, M. Hermle, and J. Goldschmidt, "Stark level analysis of the spectral line shape of electronic transitions in rare earth ions embedded in host crystals," New J. Phys. **15**(5), 053033 (2013).
11. S. Fischer, J. C. Goldschmidt, P. Loper, G. H. Bauer, R. Bruggemann, K. Krämer, D. Biner, M. Hermle, and S. W. Glunz, "Enhancement of silicon solar cell efficiency by upconversion: Optical and electrical characterization," J. Appl. Phys. **108**(4), 044912 (2010).

#202802 - $15.00 USD Received 9 Dec 2013; revised 7 Feb 2014; accepted 7 Feb 2014; published 24 Feb 2014

12. S. Fischer, A. Ivaturi, B. Frohlich, M. Rudiger, A. Richter, K. W. Krämer, B. S. Richards, and J. C. Goldschmidt, "Upconverter silicon solar cell devices for efficient utilization of sub-band-gap photons under concentrated solar radiation," IEEE J. Photovoltaics **4**(1), 183–189 (2014).
13. C. Gueymard, D. Myers, and K. Emery, "Proposed reference irradiance spectra for solar energy systems testing," Sol. Energy **73**(6), 443–467 (2002).
14. J. Handy and T. Peterson, "Concentrating PV survey: an unbiased overview," in *SPIE Solar Energy + Technology*, (International Society for Optics and Photonics, 2011), 810808–810808–810811.
15. D. Cooke, P. Gleckman, H. Krebs, J. O'Gallagher, D. Sagie, and R. Winston, "Sunlight brighter than the sun," Nature **346**(6287), 802 (1990).
16. G. E. Arnaoutakis, J. Marques-Hueso, T. K. Mallick, and B. S. Richards, "Coupling of sunlight into optical fibres and spectral dependence for solar energy applications," Sol. Energy **93**, 235–243 (2013).
17. J. M. Gordon, E. A. Katz, D. Feuermann, and M. Huleihil, "Toward ultrahigh-flux photovoltaic concentration," Appl. Phys. Lett. **84**(18), 3642–3644 (2004).
18. E. A. Katz, J. M. Gordon, and D. Feuermann, "Effects of ultra high flux and intensity distribution in multi junction solar cells," Prog. Photovolt. Res. Appl. **14**(4), 297–303 (2006).
19. P. Gibart, F. Auzel, J.-C. Guillaume, and K. Zahraman, "Below brand-gap IR response of substrate-free GaAs solar cells using two-photon up-conversion," Jpn. J. Appl. Phys. **35**(8), 4401–4402 (1996).
20. A. Slade and V. Garboushian, "27.6% efficient silicon concentrator solar cells for mass production," in *Technical Digest, 15th International Photovoltaic Science and Engineering Conference, Beijing*, 2005)
21. C. Algora, E. Ortiz, I. Rey-Stolle, V. Diaz, R. Pena, V. M. Andreev, V. P. Khvostikov, and V. D. Rumyantsev, "A GaAs solar cell with an efficiency of 26.2% at 1000 suns and 25.0% at 2000 suns," IEEE Trans. Electron. Dev. **48**(5), 840–844 (2001).
22. C. Strümpel, "Application of erbium-doped up-converters to silicon solar cells," Doctoral Thesis (Universität Konstanz, Konstanz, Germany, 2007).
23. J. C. Goldschmidt, P. Loper, S. Fischer, S. Janz, M. Peters, S. W. Glunz, G. Willeke, E. Lifshitz, K. Krämer, and D. Biner, "Advanced upconverter systems with spectral and geometric concentration for high upconversion efficiencies," in *Optoelectronic and Microelectronic Materials and Devices, 2008. COMMAD 2008. Conference on*, (IEEE, 2008), 307–311.
24. A. Mohr, M. Steuder, A. Bett, and S. Glunz, "Silicon concentrator cells designed for a direct mounting on compound parabolic concentrator," in *Photovoltaic Energy Conversion, 2003. Proceedings of 3rd World Conference on*, (IEEE, 2003), 841–844.
25. A. Mohr, "Silicon concentrator cells in a two-stage photovoltaic system with a concentration factor of 300×," Doctoral Thesis (Albert-Ludwigs-Universität, Freiburg im Breisgau, Germany, 2005).
26. A. Mohr, T. Roth, and S. W. Glunz, "BICON: high concentration PV using one axis tracking and silicon concentrator cells," Prog. Photovolt. Res. Appl. **14**(7), 663–674 (2006).
27. M. Rüdiger, S. Fischer, J. Frank, A. Ivaturi, B. S. Richards, K. W. Krämer, M. Hermle, and J. C. Goldschmidt, "Bifacial n-Type Silicon Solar Cells for Upconversion Applications," Sol. Energy Mater. Sol. Cells.
28. K. W. Krämer, D. Biner, G. Frei, H. U. Gudel, M. P. Hehlen, and S. R. Luthi, "Hexagonal sodium yttrium fluoride based green and blue emitting upconversion phosphors," Chem. Mater. **16**(7), 1244–1251 (2004).
29. W. Welford and R. Winston, *High Collection Nonimaging Optics* (Academic Press, San Diego, 1989).
30. M. A. Green, K. Emery, Y. Hishikawa, W. Warta, and E. D. Dunlop, "Solar cell efficiency tables (version 43)," Prog. Photovolt. Res. Appl. **22**(1), 1–9 (2014).
31. J. M. Bennett and E. Ashley, "Infrared reflectance and emittance of silver and gold evaporated in ultrahigh vacuum," Appl. Opt. **4**(2), 221–224 (1965).
32. J. P. Zinter and M. J. Levene, "Maximizing fluorescence collection efficiency in multiphoton microscopy," Opt. Express **19**(16), 15348–15362 (2011).
33. J. P. Rice, Y. Zong, and D. J. Dummer, "Spatial uniformity comparison of two nonimaging concentrators," Opt. Eng. **36**(11), 2943–2947 (1997).
34. S. K. MacDougall, A. Ivaturi, J. Marques-Hueso, K. W. Krämer, and B. S. Richards, "Ultra-high photoluminescent quantum yield of β-$NaYF_4$: 10% Er^{3+} via broadband excitation of upconversion for photovoltaic devices," Opt. Express **20**(S6), A879–A887 (2012).
35. F. Pellé, S. Ivanova, and J.-F. Guillemoles, "Upconversion of 1.54 μm radiation in Er^{3+} doped fluoride-based materials for c-Si solar cell with improved efficiency," EPJ Photovoltaics **2**, 20601 (2011).
36. A. Boccolini, R. Faoro, E. Favilla, S. Veronesi, and M. Tonelli, "BaY_2F_8 doped with Er^{3+}: An upconverter material for photovoltaic application," J. Appl. Phys. **114**(6), 064904 (2013).
37. R. Winston, J. C. Miñano, and P. G. Benitez, *Nonimaging Optics* (Academic Press, Amsterdam; Boston, Mass., 2005).
38. R. Abram, R. Allen, and R. Goodfellow, "The coupling of light emitting diodes to optical fibers using sphere lenses," J. Appl. Phys. **46**(8), 3468–3474 (1975).

1. Introduction

Up-conversion (UC) is a promising third generation photovoltaics (PV) approach for overcoming the Shockley-Queisser (SQ) limit [1], which restricts the conversion efficiency of single junction silicon solar cells to 29.4% [2]. UC targets the reduction of the transmission

#202802 - $15.00 USD Received 9 Dec 2013; revised 7 Feb 2014; accepted 7 Feb 2014; published 24 Feb 2014

losses resulting from photons with energy less than the band-gap of the solar cell. Harvesting of these sub-band-gap photons has been predicted to be able to enhance the conversion efficiency limit of a silicon solar cell to 40.2% and 53.0%, under one-sun and 46,200 suns, respectively [3].

UC in rare earth ions doped in oxide, fluoride, bromide and chloride hosts has been analyzed and documented extensively [4–6]. For PV, trivalent erbium (Er^{3+}) in hexagonal sodium yttrium fluoride (β-$NaYF_4$) is one of the most promising UC candidates [7] and has been reported and applied for use with silicon solar cells [8–10]. UC occurs between the intra *4f-4f* transitions in Er^{3+} via the following possible routes depicted graphically in Fig. 1. Long wavelength photons (1450-1590 nm) are absorbed via ground state absorption (GSA) from the $^4I_{15/2}$ level to the $^4I_{13/2}$ metastable level in the Er^{3+} ion. From this level, two UC processes are possible. Firstly, after absorption of a second photon via excited state absorption (ESA), the ion reaches the $^4I_{9/2}$ level where due to the low lifetime relaxes non-radiatively to the $^4I_{11/2}$ level. A second, and more probable process, occurs after GSA at the $^4I_{13/2}$ level between two neighboring Er^{3+} ions where the energy from one ion is transferred to the other, leading to energy transfer up-conversion (ETU) to the $^4I_{9/2}$ for the high energy ion, and to the ground state for the low energy ion. Again, the $^4I_{9/2}$ level relaxes non-radiatively to the $^4I_{11/2}$ level. From this level the ion relaxes radiatively to the ground state via emission of a photon with energy equal to the ΔE (980 nm peak wavelength emission).

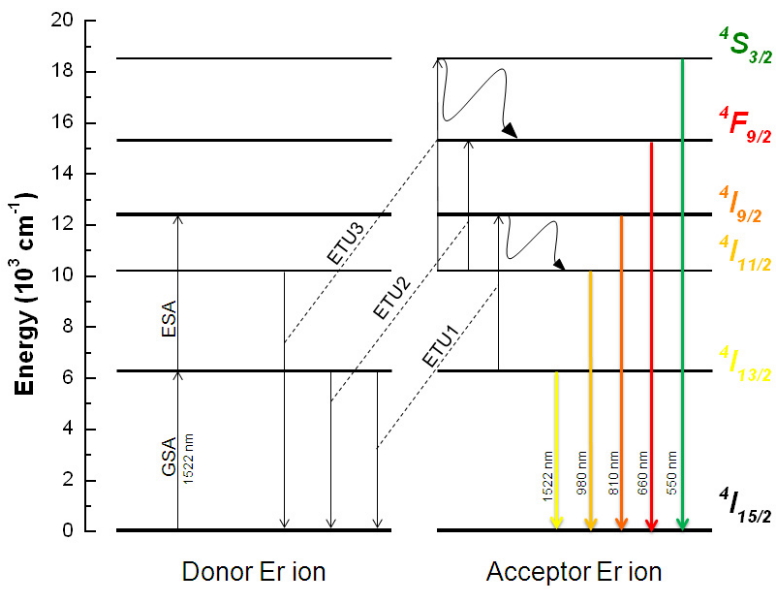

Fig. 1. Transitions in Er^{3+} responsible for up-conversion for photovoltaics. Upward solid lines represent absorption, downward solid lines represent emission, dotted lines represent energy transfer up-conversion and non-radiative relaxation is depicted by curved lines.

This two-photon nature of these processes leads to the non-linear behavior of UC devices with incident power. Reports in the literature on UC-PV devices based on $NaYF_4$:Er, have been characterized for power densities in the range of 1000 W/m^2 [11, 12]. This power density is monochromatic and does not correspond to 1 sun, which is the integrated power density over the air-mass 1.5 global (AM1.5G) solar spectrum [13]. To achieve this, with the monochromatic power density per wavelength at the range 1450-1600 nm available in the AM1.5G solar spectrum (~0.28 W/m^2/nm), a system of approximately 3500 × the available power density is required. These levels of solar concentration are likely to be utilized in high

#202802 - $15.00 USD Received 9 Dec 2013; revised 7 Feb 2014; accepted 7 Feb 2014; published 24 Feb 2014

concentrating photovoltaic (CPV) systems designed to operate in the range of 500-1,200 suns [14], while a record of 84,000 suns has been experimentally demonstrated on earth [15]. Although none of the stated solar concentrations specify the concentration as a function of wavelength, it should be noted that this relationship is not always constant, especially for CPV systems with secondary optics which are spectrally dependent [16]. In addition, this concentration is an average value, as the spatial distribution can vary significantly depending on the geometry of the optics, resulting in higher local concentrations useful for UC, but undesirable for the solar cell.

State-of-the-art solar cells are not designed to operate efficiently under such high concentrations due to large series resistance losses that lead to thermal management issues [17, 18]. As a consequence, the layered device configuration firstly demonstrated by Gibart *et al.* on GaAs cells [19] and later on silicon cells by Shalav *et al.* [8], will lead to operation of the cell at a low efficiency regime. For comparison, the highest demonstrated conversion efficiency for silicon cells is at 100 suns [20] and for GaAs at 1000 suns [21]. Therefore, a mismatch exists between the optimal concentration for the solar cells and that for the UC material. As a direct consequence, an up-conversion photovoltaic (UC-PV) device with secondary concentration of the sub-band-gap photons is a promising approach. To the best of the authors' knowledge, two reports were found in literature relating to secondary concentration directly on the UC layer. The first was proposed by Strümpel *et al.* [22] with localized application of UC material at the back of solar cells and geometrical concentration at the range of 2 × utilized by slanted metalized rear contacts. The second was proposed by Goldschmidt *et al.* [23] with a luminescent solar concentrator (LSC) at the rear of the UC layer to increase the solar and spectral concentration of sub-band gap photons. In this UC-PV system, a low solar concentration of approximately 10 suns is predicted by the LSC and spectral concentration by incorporation of near-infrared (NIR) emitting quantum dots to broaden the absorption spectrum of the UC layer.

In this paper, we incorporate concentrating optics on the rear side of a bifacial silicon solar cell, with the intention to further concentrate only the sub-band-gap photons useful for UC as shown in the schematic in Fig. 2(a). In this manner, the solar cell can operate at a more suitable concentration to maximize its conversion efficiency, while the transmitted light is further concentrated to the high power densities required for efficient UC. After further integration with primary optics, the UC-PV device could be fully associated with CPV systems. This route proposes the research questions of, firstly, what effect does the addition of secondary concentration optics have on the NIR response of an UC-PV device, and secondly how do different concentrator geometries affect the performance of the integrated UC-PV device.

2. Materials and methods

Rear-line-contacted-concentrator (RLCC) silicon cells were used to realize the UC-PV device. The cells were based on a design originally intended for CPV systems with maximum efficiency optimized at 100 suns [24–26], however these were modified to be both planar and bifacial. The best cell used in this study had an efficiency of 14% under 1 sun and external quantum efficiency (EQE) of 38% at 980 nm. It should be noted that for future research on the integration of UC-PV devices into systems, solar cells that have been recently specifically designed for this purpose [27] would offer significant advantages.

The concentrating integrated optics consist of two different dielectric tapers made of fused silica with refractive index $n = 1.46$ at $\lambda = 589$ nm as described in reference [16] (labeled 2 and 3) with effective acceptance half-angles 10.50° and 17.16°, respectively. Bare (uncoated) tapers were experimented with, as well as applying gold (Au) coatings (~240 nm minimum thickness) on the external surface of the tapers by plasma sputter-coating (Fisons Instruments, Polaron SC502). Additional optical elements used in this study for comparison were an objective lens (Leitz Wetzlar, NPL100) with magnification 100 × , numerical aperture (*NA*) of 1.30, entry and exit apertures 28.26 mm^2 and 3.14 mm^2 respectively, and a parabolic concentrator made in-house from fused silica, with entry and exit apertures 107.64 mm^2 and 46.42 mm^2, respectively. A schematic of the configurations is depicted in Fig. 2(a) and photo of the parabolic concentrator attached with the bifacial solar cell is shown in Fig. 2(b). An ultraviolet/visible/NIR spectrometer (Perkin Elmer, Lambda 950) has been used for transmission measurements, equipped with an integrating sphere to support solid angles up to 2π sr from the exit apertures of each optical element.

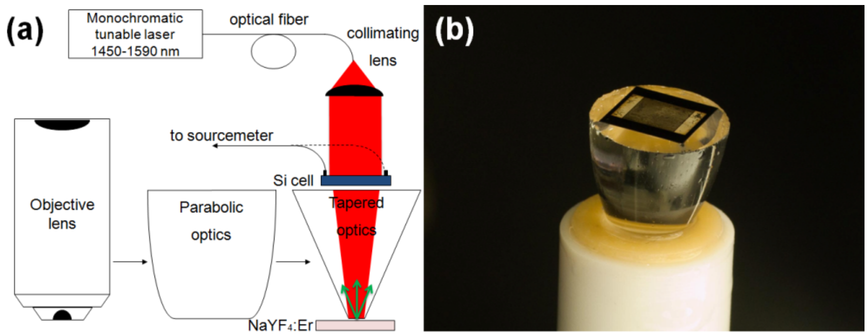

Fig. 2. (a) Schematic of the UC-PV device with integrated optics behind the solar cell. For detailed characteristics the reader is referred to section 2, materials and methods. (b) One of the concentrators used in this study (parabolic) with a bifacial silicon solar cell attached. The UC phosphor is attached on the exit aperture of the parabolic concentrator.

The β-$NaYF_4$ microcrystalline powder with 25% Er^{3+} doping concentration used in this study was prepared following the method described by Krämer *et al.* [28]. The powder was cast in a perfluorocyclobutane (PFCB) polymer (Tetramer Technologies LLC, USA) matrix at a phosphor to polymer weight ratio of 84.9%. Optical coupling between elements was achieved with refractive index matching liquid (Cargille, L-RIA-766, n = 1.53 at λ = 589.2 nm) applied between the interfaces of the UC-PV device in limited quantity to avoid affecting the wave-guiding properties of the integrated optics.

The UC-PV system was illuminated at normal incidence with a NIR tunable laser (HP-Agilent, 8168-F, 6 mW at 1522 nm) covering a wavelength range of 1450-1590 nm. The laser was fiber-coupled and collimated, resulting in a beam with a second moment width diameter ($d4\sigma$) of 4.2 mm and a divergence half-angle of 0.02^o, characterized with a NIR camera (Electrophysics, Micronviewer 7290A). The photocurrent generated from the solar cell was measured with a sourcemeter (Keithley Instruments, 2440-C) and the power incident on the device was measured using a calibrated germanium photodiode (Newport, 818-IR). For the power density at the UC phosphor, the same illumination system was used, but the phosphor at the output of each optic has been replaced with an integrating sphere attached with the germanium photodiode, both calibrated for the excitation wavelength (1522 nm). The EQE of the device was calculated after acquisition of the generated short-circuit current I_{sc} and incident power P_{in} using the following relationship:

$$EQE = \frac{hcI_{sc}}{\lambda e P_{in}}, \tag{1}$$

where h is Planck's constant in m^{2}kg/s, c the speed of light in m/s, λ the excitation wavelength in m and e the electronic charge in coulombs.

3. Results and discussion

Each of the optical elements in this study encompasses different concentrating properties and has been selected for the following reasons. The tapered concentrators, although non-ideal compared to the parabolic concentrator, feature significantly higher concentration ratios –

28.7 × and 33.7 × for tapers 2 and 3, respectively. The parabolic concentrator although having a lower concentration ratio of 2.3 × , is considered thermodynamically an ideal concentrator and its angular acceptance is superior to the tapers [29]. This last attribute plays a significant role on high CPV systems which are normally combined with primary optics. Last, the objective lens was also used to obtain a comparison of optics with higher concentration of 100 × . As discussed in the introductory section, the non-linear nature of UC, requires an UC-PV system in the range of 3500 × solar concentration. With the assumption that silicon solar cells can operate at 100 suns (which is valid with state-of-the-art silicon solar cells [20] if characterized under standard temperature and illumination conditions [30]), the secondary optics should concentrate the transmitted sub-band-gap photons 35 × to acquire the required solar concentration for UC. Therefore a range of possible solar concentrations around this value is covered with the selected secondary optics.

The EQE of the UC-PV device with five different secondary concentrating optical elements is shown in Fig. 3 as a function of the excitation wavelength at a power density of 0.007 W/cm^2. The spectra are similar in shape, with the highest EQE observed for all three devices at 1522 nm, while secondary resonant peaks are observed at 1508 nm and 1497 nm. The line shape of the spectra follow also with minor peaks at 1473 nm, 1543 nm, 1551 nm and 1564 nm, resulting from the convolution of the Stark levels with energy between 5500 cm^{-1} and 7500 cm^{-1} [10].

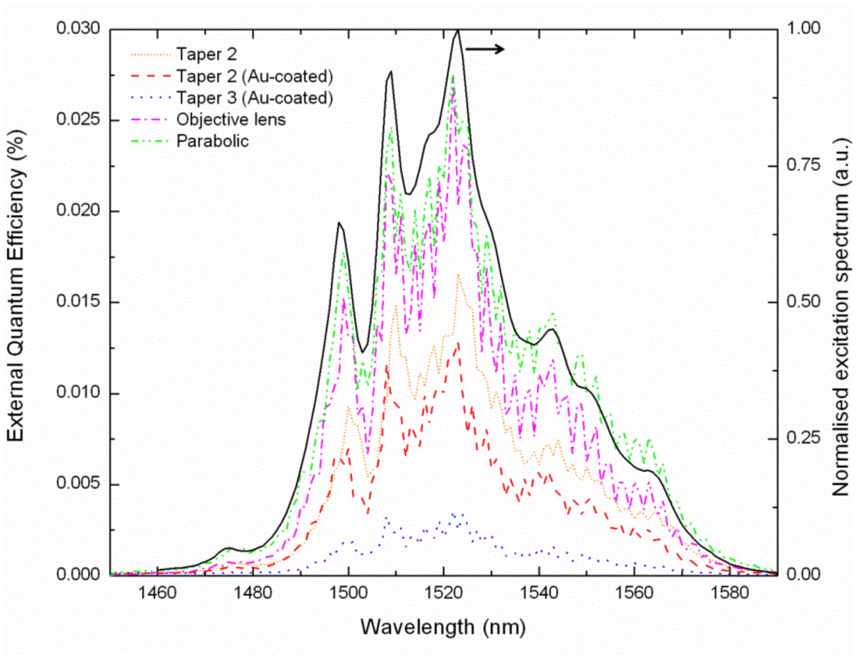

Fig. 3. EQE of UC-PV device characterized between 1450 and 1590 nm at 0.007 W/cm^2 with five different secondary concentrator elements. The EQE closely resembles the $^4I_{15/2}$ to $^4I_{13/2}$ excitation spectrum of Er^{3+} shown on the secondary axis with main resonant peaks at 1497, 1508, 1522 nm.

The highest EQE was measured with the parabolic concentrator, while a lower EQE was obtained with the objective lens despite its higher concentration ratio and entry aperture matching the area of the solar cell. An even lower EQE was measured with taper 2 due to optical losses associated with disruption of total internal reflection (TIR). The EQE did not improve even when the tapers were coated with Au. On the contrary, as demonstrated in Fig. 3, a reduced EQE response was observed after coating taper 2. The reflectivity of Au at ± 5^o

angle of incidence for both the excitation (1450-1590 nm) and emission (940-1050 nm) wavelengths is greater than 99% [31], however this value would be multiplied for every reflection resulting in a factor of R^{n+m}, where R the reflectivity at the interface, n and m the number of reflections for the excitation and emission respectively. This is expected to affect the excitation at normal incidence, but especially the internal reflection of the isotropic UC emission. The EQE of the device with taper 2 shows a higher response than with taper 3. As taper 3 has a higher angle of acceptance than taper 2, a progressively higher angle of reflection and consequently a higher number of reflections n, before the excitation reaches the β-$NaYF_4$:Er up-converter.

The response of each device is described on the one hand by the optical losses due to transmission of the excitation (named here also forward transmission), and on the other hand by losses due to transmission of the UC emission back to the solar cell (named backwards transmission). To estimate the losses due to excitation, each optical element was characterized for forward transmission between wavelengths of 900 nm and 1600 nm (Fig. 4). As mentioned in the section of materials and methods, the exit aperture of the optical elements was positioned flush with the entrance port of an integrating sphere to make possible measurement over a solid angle of 2π sr. The transmission is constant within 1% for this wavelength range as expected for the material of the optical elements (fused silica). A reduced transmission is observed between elements with 82% for the parabolic concentrator, 77% for the objective lens and 65% for the Au-coated taper 2 at 1522 nm; the wavelength where the highest EQE was obtained. For comparison, the transmission of the bifacial solar cell is also plotted in Fig. 4, with 42% at 1522 nm.

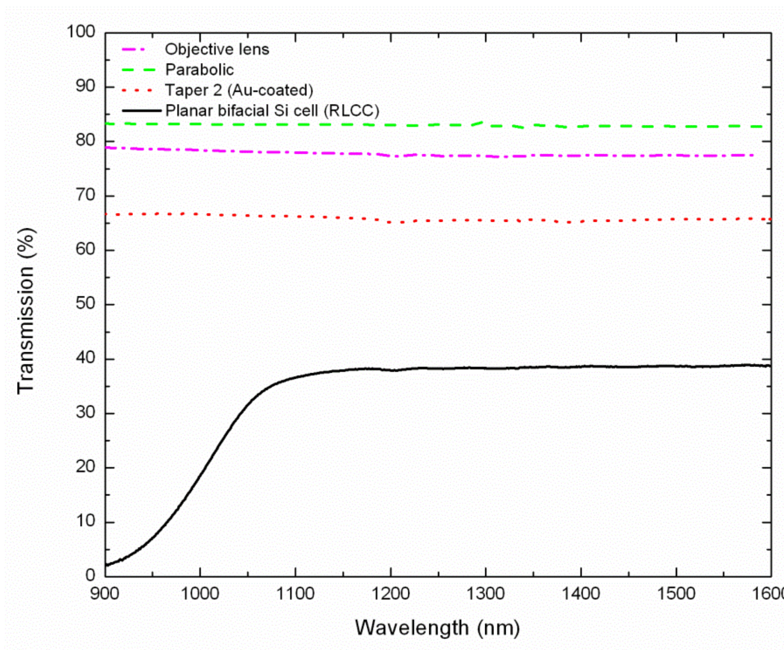

Fig. 4. Transmission of the concentrating elements of the UC-PV device as a function of wavelength between 900 and 1600 nm. The transmission of the bifacial solar cell is also plotted for comparison.

The transmission between optical elements follows the same trend as the EQE of each UC-PV device, which suggests that a significant portion of the optical losses in the UC-PV device originates from reduced transmission of the excitation.

The losses due to backwards transmission can be estimated based on the light collection properties of the optical elements. For an objective lens this collection over a solid angle 2π is described by the NA and the refractive index of the immersion medium n from the following equation,

$$\left(1-\sqrt{1-\left(\frac{NA}{n}\right)^2}\right). \tag{2}$$

For the parabolic and tapered optics the backwards transmission was determined by Monte Carlo simulations. The isotropic emission at the main wavelength of 980 nm was modeled as a Lambertian source extending over 2π. These results are shown in Fig. 5 for source diameters between fully covering the exit aperture of the optics (7.69 mm for the parabolic and 2 mm for the tapered optics) and down to 1μm.

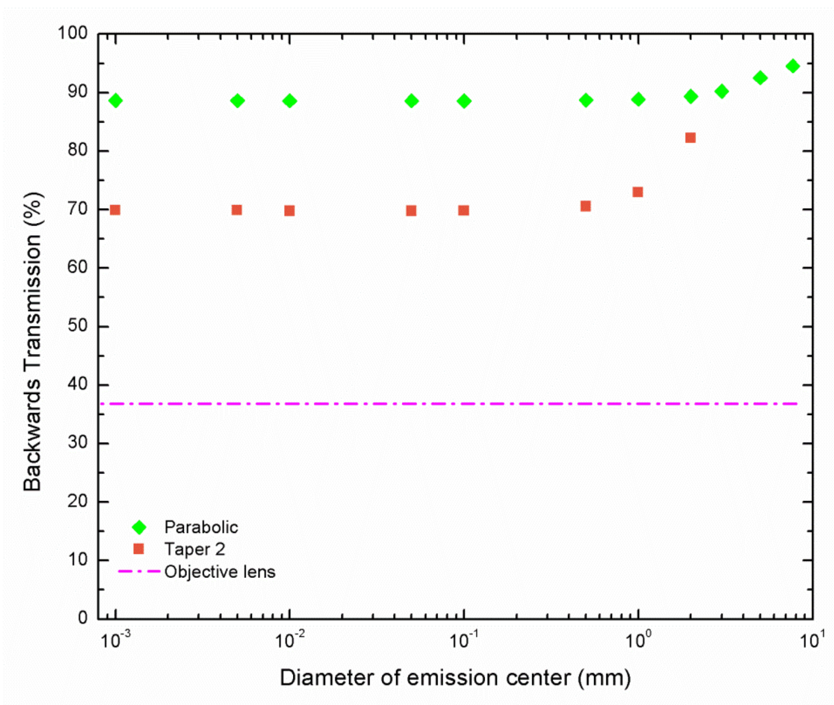

Fig. 5. Backwards transmission of the concentrating elements of the UC-PV device as a function of the diameter of an isotropic emission center. The transmission of the objective lens, estimated from Eq. (2), is plotted for comparison.

A backwards transmission higher than 88% is revealed for the parabolic optics, while 69% is given for taper 2. The transmission of both parabolic and tapered optics is displayed to be higher as the diameter of the emission center approaches the diameter of the aperture of the optics. As the diameter of the source increases, the angle of reflection traced from the Lambertian emitter to the edge of the optic is smaller, resulting in progressively higher backwards transmission. While the parabolic concentrator displays high collection properties for the emission, the collection efficiency of the objective lens is limited by its geometry to only 47%. This efficiency is multiplied by the forward transmission to result to a 36% backwards transmission. While this value might appear low compared to the parabolic and tapered optics, it agrees well with dedicated studies on objective lenses [32], where collection and transmission of fluorescence is crucial for multi-photon microscopy.

The forward transmission is expected to affect the population rates of β-$NaYF_4$:Er in the UC layer, while the backwards transmission is expected to affect the collection of the UC emission, and consequently the EQE of the UC-PV device. Therefore a power dependent characterization of the UC-PV is needed to further investigate this effect. As the highest EQE was observed for an excitation wavelength of 1522 nm, the incident power at this wavelength was varied to obtain the EQE as a function of excitation power. These results are displayed in Fig. 6 for all UC-PV devices.

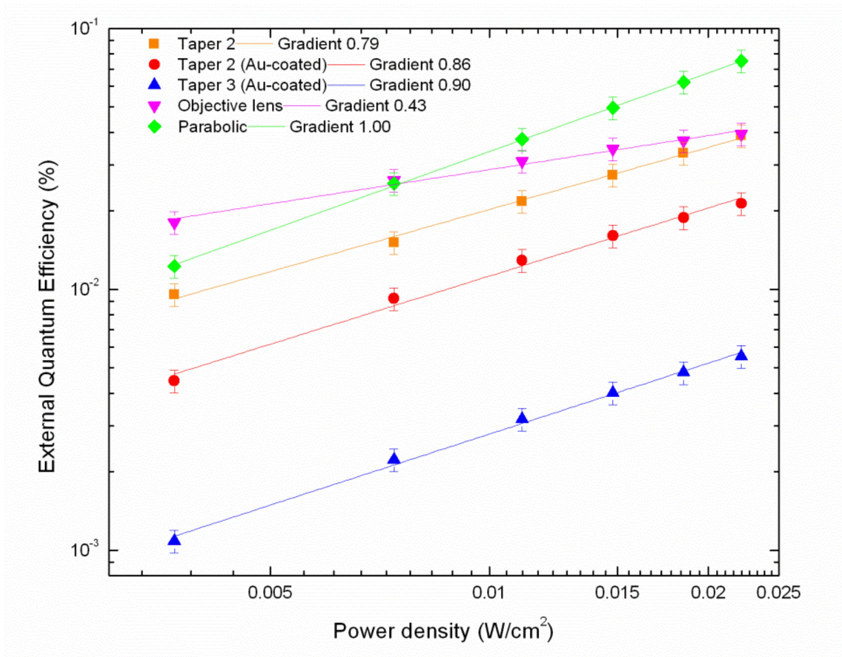

Fig. 6. Power dependent EQE of the PV-UC device for the strongest resonant peak at 1522 nm. The gradient of each least square fit indicates the order of the luminescence process involved on each device.

An EQE of 0.038% was obtained with uncoated taper 2, while this value was reduced by half following Au deposition. As expected the EQE of the device with the parabolic optics performed best with a maximum EQE of 0.075% under excitation of 0.022 W/cm^2, while under the same excitation power, the EQE of the UC-PV with the objective lens was 0.039%. A lower EQE of 0.006% was obtained for the Au-coated taper 3 as expected due to the optical losses described previously.

The power dependence of non-linear optical processes is commonly plotted on double logarithmic scales to extract information about the number of excitation photons involved in UC emission and consequently the order of UC. In an UC-PV device, the UC emitted photons are measured directly by the solar cell and follow a quadratic relation between I_{sc} and power density [8]. Therefore, from Eq. (1), the EQE follows a relation with power density of the form:

$$EQE \propto \frac{P^n}{P} \propto P^{n-1}, \tag{3}$$

where the exponent n is the order of UC. As shown in Fig. 6, the gradient of the least square fit is 1.00 for the UC-PV device with parabolic concentrator which agrees with Eq. (3) for n = 2, i.e. two-photon UC. For the UC-PV devices with taper 2, Au-coated taper 2 and Au-coated taper 3, the gradient is 0.79, 0.86 and 0.90 respectively which suggests that mechanisms such

#202802 - $15.00 USD Received 9 Dec 2013; revised 7 Feb 2014; accepted 7 Feb 2014; published 24 Feb 2014

as excitation of higher energy levels, cross relaxation or amplified spontaneous emission are more probable and are competing with ETU and ESA [5]. The gradient is reduced further from the theoretical down to 0.43 for the UC-PV system with objective lens with the highest concentration ratio of all devices in the study.

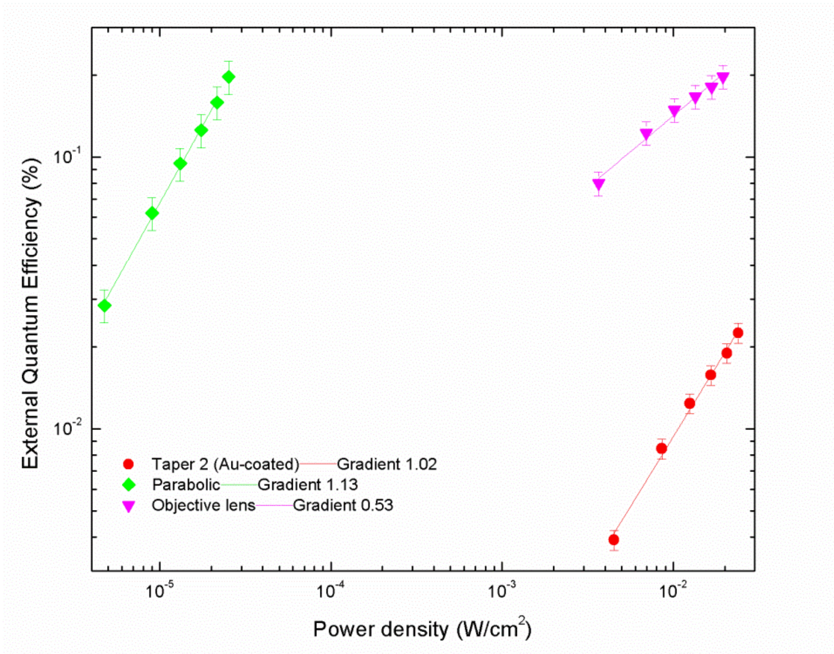

Fig. 7. EQE of the PV-UC device for the resonant peak at 1522 nm at the UC layer. The power density on the UC layer and the respective regime, achieved by each concentrator, is indicated by the gradient.

Although the EQE of each UC-PV device has been displayed in Fig. 6 for equal incident power densities, the power density on the UC layer should be quantified to indicate the achievable concentration that actually excites the UC. As shown in Fig. 7, where the EQE is plotted as a function of the power density on the UC layer (measured after the solar cell and the concentrating optics), the power density is adjusted for the lower and high-pump regimes. In particular, the power density achieved with the parabolic optics remains in the low-pump regime with gradient 1.13 while the objective lens is at the high-pump regime with a gradient of 0.53. It is noted that the output of the parabolic concentrator wasn't totally illuminated; therefore the power density is expected to be higher in the case of full illumination. Despite this, the EQE resulting from the parabolic concentrator indicates the suitability of the optics for collection of the emission back to the solar cell. Although the tapered optics achieve power densities as high as the objective lens, the gradient remains on the low-pump regime with gradient of 1.02 which can be explained by poor collection of the emission with a backwards transmission of 70% back to the solar cell.

By comparing the power density in Fig. 7 with the power density from independent measurements [7] of the UC quantum yield for the same UC phosphor, it is shown that the gradients leading to saturation at the high-pump regime observed here appear in lower powers. While this power is an average of the achieved concentration at the UC layer, the geometry of each concentrating optic is known to have a non-uniform profile [33] that may lead to much higher local power densities. This effect was investigated further by Monte Carlo simulations for the parabolic and tapered optics and is displayed in Fig. 8.

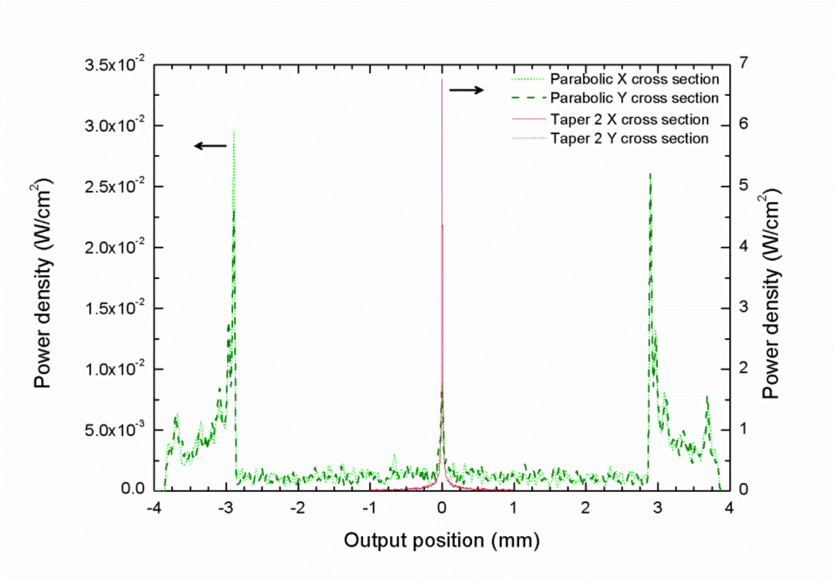

Fig. 8. Irradiance profile at the output of the parabolic and the tapered optics. Localized peak concentrations are observed for both, that are responsible for the gradient of the least square fits in Figs. 6 and 7.

The available power from the fiber-coupled laser after the solar cell was used to illuminate the entry apertures of the optics. As shown in Fig. 8, the irradiance profile at the output of the parabolic concentrator is uniform at the center, but exhibits local concentration towards the edges of the aperture that reach power densities as high as $3x10^{-2}$ W/cm^2. Highly local concentration is also displayed for the tapered concentrator, at the center of the exit aperture with values as high as 6.50 W/cm^2.

An experimental demonstration wasn't allowed, due to distortion of the output profile measured with an IR camera, originating from the optics used to expand the laser beam. An irradiance profile similar to the taper is expected also for the objective lens. Again, this could not be verified experimentally due to the aforementioned reasons and additionally due to the high *NA* of the objective lens.

For increasing power density at the UC layer, an inverse relation is observed for the gradient, that is the order of UC. It is known that for incident power densities in the high-pump regime (1000 W/m^2,) the slope of the relationship between power density and the UC emission is 0.35 [11]. Thus, for a given system, the EQE can saturate at a certain high value of power density. These findings agree very well with our results. Higher power densities at the UC layer, are also associated with a higher UC quantum yield [7, 34]. Therefore, where lower gradients do not correlate with a higher EQE (as is the case for tapered optics) this is a sign for optical losses in the backward transmission. However, the results confirm the initial hypothesis for independent optimization of the sub-band-gap photons, since for a constant power density incident on the UC-PV device, the concentration on the UC layer can be optimized to levels that maximize UC.

The normalized EQE (NEQE) for the highest power density of 0.022 W/cm^2 is listed in Table 1 for the five devices of the study along with the UC-PV devices based on Er^{3+} found in literature for comparison. A value of $3.38x10^{-2}$ cm^2/W was calculated for the device using the parabolic concentrator. The NEQE of the device in this work is comparable with the other devices found in literature [8, 9, 11, 12, 35, 36]. It is mentioned that the NEQE of the device without any concentrating optics was $13.15x10^{-2}$ cm^2/W, higher than the NEQE of the best

UC-PV device of the study with the parabolic concentrator, which is reflecting the optical losses discussed previously.

Table 1. Comparison of UC-PV Devices Based on Er^{3+} with Aabsolute and Normalized EQE

	UC phosphor	λ (nm)	EQE (%)	W/cm^2	NEQE (cm^2/W)	Reference
	$NaYF_4:Er^{3+}$(20%)	1523	2.5	-	-	[8]
	$NaYF_4:Er^{3+}$(20%)	1523	3.4	2.4	1.40 x 10^{-2}	[9]
	$NaYF_4:Er^{3+}$(20%)	1522	0.34	0.109	3.00 x 10^{-2}	[11]
	$CaF_2YF_3:Er^{3+}$(5%)	1540	2.4	100	0.024 x 10^{-2}	[35]
	BaY_2F_8: Er^{3+}(30%)	1557	5.1	2.4	2.10 x 10^{-2}	[36]
	$NaYF_4:Er^{3+}$(20%)	1508	1.79	0.1	17.9 x 10^{-2}	[12]
$NaYF_4:Er^{3+}$	Taper 2	1522	0.038	0.022	1.75 x 10^{-2}	This study
	Taper 2 (Au-coated)	1522	0.021	0.022	0.96 x 10^{-2}	
	Taper 3 (Au-coated)	1522	0.005	0.022	0.24 x 10^{-2}	
	Objective lens	1522	0.039	0.022	1.77 x 10^{-2}	
	Parabolic	1522	0.075	0.022	3.38 x 10^{-2}	

The EQE values reported in this study are low for a functional UC-PV device, however they were acquired with integrated optics that have not been optimized for forward and backward transmission. Despite this, the proof-of-principle experiments have shown that the presented devices enhance the sub-band-gap response of a silicon solar cell without prior concentration.

There are several points signified by the results of this work that can be indicated for further optimization of the UC-PV device:

- Transmission of the solar cell: The bifacial solar cell used in this study has exhibited poor spectral response at 980 nm and 42% transmission at 1522 nm. It is clear that with the current progress in solar cells for UC-PV devices with optimized reflection and transmission at the wavelength of excitation [27] and a reported NEQE of $17.9 x 10^{-2}$ cm^2/W [12], a significant enhancement of the NEQE is expected for the proposed UC-PV devices.
- Optics for excitation: The transmission of the concentrating optics in this study exhibited a direct effect on the EQE of the UC-PV devices. However, the optical elements used in this study were selected according to their concentrating properties and not the absolute transmission. Refracting and TIR optics displayed better performance to coated reflecting optics in this study, although the incident excitation reaching the UC depends on the irradiance profile and the localized concentration.
- Optics for UC emission: Concentrating optics are in general designed for forward transmission. In the case of the proposed UC-PV device the exit aperture of the optics is also the entry aperture for a source with isotropic emission (the UC layer). Optics that fulfill the last property have been extensively studied [37] and lessons can be learned from the optics of light-emitting-diodes [38]. However, the backwards transmission of the parabolic optics was shown to be superior to the other optics of the study, exhibiting efficient collection of the extended isotropic emission.
- Concentration ratio: It has been shown that the concentration ratio of the secondary integrated optics plays a significant role on the EQE of the UC-PV. Although low to moderate concentration levels can be adequate to maximize UC emission, higher concentration will populate higher energy levels and competing processes that lead to reduced UC. In addition, the irradiance profile at the output of the concentrator can vary significantly from the geometric concentration and exhibits localized peaks that further enhance saturation effects. Finally this secondary concentration should be matched with adequate primary concentration at levels that maximize the

#202802 - $15.00 USD Received 9 Dec 2013; revised 7 Feb 2014; accepted 7 Feb 2014; published 24 Feb 2014

efficiency of the PV layer. It is therefore envisaged that the elements that assemble the UC-PV device are optimized concurrently in order for this technology to have a direct effect.

4. Conclusions

In this paper concentrating optics were integrated in UC-PV devices to investigate the effect of independent solar concentration of sub-band-gap photons. The concentration was achieved by dielectric tapered, parabolic and imaging optics. The Au-coated tapers exhibit lower response compared to the uncoated as a result of the multiple reflections of the excitation before reaching the UC layer. The UC-PV device with parabolic concentrators results in the highest EQE of the study of 0.075%, corresponding to a normalized EQE of 3.38×10^{-2} cm^2/W, achieved without prior concentration of the excitation incident on the device. This result indicates that solar concentration of the sub-band-gap photons can be independently optimized and represents a significant step for UC-PV devices towards integration in CPV systems.

Acknowledgments

This work was financially supported by the Engineering and Physical Sciences Research Council (EPSRC) under the Luminescent Lanthanide Layers for Enhanced Photovoltaic Performance (L3EAP2) Project Agreement No. EP/I013245/1, as well as the European Community's Seventh Framework Program (FP7/2007-2013) under grant agreement No. [246200]. We are thankful to the reviewers for their insightful comments that improved significantly this body of work.